World Journal of Modelling and SimulationVol. 7 (2011) No. 1, pp. 29-39. ISSN 1 746-7233, England, UK. Submitted 19-NOV-2009, revised on 05-JAN-2010 & 01-MAY-2010, accepted on 07-JUN-2010, published online 28-JAN-2011:
http://www.wjms.org.uk/wjmsvol07no01paper03.pdf

An Effective Simulated Annealing Refined Replica Exchange Markov Chain Monte Carlo Algorithm for the Infectious Disease Model of H1N1 Influenza Pandemic

Jiapu Zhang
Centre for Informatics and Applied Optimization & Graduate School of ITMS, The University of Ballarat, Mount Helen, Ballarat, VIC 3353, Australia
Mobile: (61) 423 487 360, E-mail: jiapu_zhang@hotmail.com, j.zhang@ballarat.edu.au

Abstract: This paper is concerned with a computational algorithm for fitting a deterministic MSEIRS (immune-susceptible-exposed-infectious-recovered-susceptible) epidemic model for the transmission of influenza (H1N1) to mortality data. The model-fitting is carried out using a simulated annealing refined replica exchange Markov chain Monte Carlo algorithm. The effectiveness of the algorithm is illustrated using the triple wave data from five English towns collected during the 1918-19 influenza pandemic. Numerical results show that the replica exchange (refined by simulated annealing) sampling technique is superior to other existing sampling techniques such as the Gibbs sampling technique, the Metropolis-Hastings sampling technique, the Multiple-try Metropolis technique for the Markov chain Monte Carlo computation. The algorithm presented in this paper has great promise to be used for carrying out some numerical computations of the current complex 2009-10 influenza pandemic.
Key words: Replica Exchange; Simulated Annealing; Markov Chain Monte Carlo; Metropolis-Hastings Sampling; Gibbs Sampling; Multiple-try Metropolis; Extended MSEIRS Model.

1 Introduction

The world is facing this century's first influenza pandemic caused by the recent outbreak of H1N1 swine influenza. In fact H1N1 swine flu pandemic once happened in multiple waves in 1918-19. A detailed epidemic model for H1N1 swine flu may be demonstrated as follows ([1, 5, 6, 9, 10, 11, 12, 17, 21, 22, 29, 31, 37]):

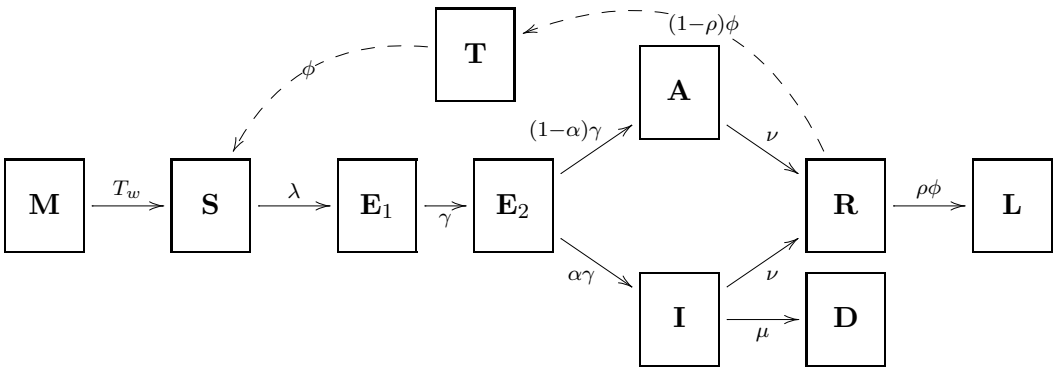

Extended MSEIRS Model. Within a period of time in resistant state (T_w) the prior immune individuals (M) become into susceptible individuals (S), then the susceptible individuals are exposed into two sequential latent infections (E_1 and E_2 with infectious rate γ) as the results of the exposure to the force of infection (λ). A proportion α then become infective and symptomatic (I, i.e. clinically ill and infectious) and a proportion 1-α become asymptomatic or unpapered infective (A). Both I and A pass to the recovered class with immunity (R) with recovery rate ν; some individuals of I class become in the death class (D) with a proportion μ of infected individuals who die. From R a proportion ρ develop longer-lasting protection (L), while the remainder pass through a temporary state (T) and eventually become into S again with $\phi = 2/T_w$.

The former achievements on MSEIRS model ([1, 5, 6, 9, 10, 11, 12, 17, 22, 29, 31, 37]) are mainly on the passively immune class M of infants. This paper extends M to the prior immune in a very general sense as in [21, 23, 24] and is concerned with a practical computational algorithm for the Extended MSEIRS Model. The prior immune (M) of this paper is not only gained from infants' mother, but also gained from seasonal influenza, vaccination, etc ([21, 23, 24] and references therein); this is a new research direction of the studies of the spread of H1N1 in the influenza pandemic, though it is not our interests of this paper.

The aim of this paper is to construct and demonstrate a computational algorithm for fitting the above extended MSEIRS epidemic model to mortality data. In Section 2 of this paper, a deterministic ordinary differential equation (ODE) mathematical model is built and a simulated annealing refined replica exchange Markov chain Monte Carlo (REMCMC) algorithm is designed. The effectiveness of the algorithm is illustrated using the triple wave data from five English towns collected during the 1918-19 influenza pandemic ([27]). The MCMC ([2, 4, 5, 15]) model-fitting algorithm is used to estimate parameter distributions of the model. The statistical sampling technique of RE ([13, 18, 19, 32, 33]) is enclosed into the MCMC algorithm, where a simulated annealing scheme ([3, 16]) is employed to refine the RE. Numerical results in Section 3 of this paper show that the simulated annealing-refined RE sampling technique is superior to the Metropolis-Hastings (MH) sampling technique ([4], from which we may know that Gibbs sampling can be rewritten as a Metropolis algorithm; thus, the RE sampling is superior to the Gibbs sampling too), the Multiple-try Metropolis (MM) sampling technique for the Markov chain Monte Carlo computation of the extended MSEIRS epidemic model. The simulated annealing refined REMCMC algorithm presented in this paper has great promise to be used for carrying out some numerical computations of the current complex 2009-10 influenza pandemic.

The organization of this paper is as follows. The ODE mathematical model for the Extended MSEIRS Model is built in Section 2, and its solver, the simulated annealing refined replica exchange Markov chain Monte Carlo algorithm, is presented in Section 2. Section 3, using the triple wave data from five English towns collected during the 1918-19 influenza pandemic, tests the algorithm for the ODE model. Numerical results are shown and discussed in Section 3. Compared with other existing sampling algorithms such as the Metropolis-Hastings algorithm (where the Gibbs sampling is its special case), the Multiple-try Metropolis algorithm, the algorithm presented in this paper is

concluded in Section 4 as a promising algorithm to be used to study the H1N1 influenza pandemic.

2 Model Building and Solving

R_0 denotes the basic reproduction number ([1, 14, 26]). We assume that the infections of A do not transmit and both A and I occur in proportion, M individuals have prior immunity including the innate immunity for children, some S individuals who were exposed in E_1 and E_2 will develop into A or I and then become into L individuals and we allow for the possibility that protection may be lost and R individuals become into S individuals again because immunity waned in individuals in waves or antigenic drift of the virus. We also assume the populations are homogeneous mixing between individuals. With these assumptions, we will build the model by the following ODEs ([5, 8, 9, 10, 12, 17, 20, 21, 22, 37]) and then solve it by the simulated annealing refined REMCMC algorithm.

2.1 An ODE Model

$$\frac{dM}{dt} = -\frac{2}{\phi}MS - \mu M \tag{1}$$

$$\frac{dS}{dt} = -\frac{R_0\nu}{N\alpha}IS + \phi T \tag{2}$$

$$\frac{dE_1}{dt} = \frac{R_0\nu}{N\alpha}IS - \gamma E_1 \tag{3}$$

$$\frac{dE_2}{dt} = \gamma E_1 - \gamma E_2 \tag{4}$$

$$\frac{dA}{dt} = (1-\alpha)\gamma E_2 - \nu A \tag{5}$$

$$\frac{dI}{dt} = \alpha\gamma E_2 - \nu I \tag{6}$$

$$\frac{dD}{dt} = \mu I \tag{7}$$

$$\frac{dR}{dt} = \nu(I+A) - \phi R \tag{8}$$

$$\frac{dT}{dt} = (1-\rho)\phi R - \phi T \tag{9}$$

$$\frac{dL}{dt} = \rho\phi R \tag{10}$$

$$M(0) = S(0) = Nz, R(0) = N(1-z), I(0) = I_0, \quad \ldots$$
$$E_1(0) = E_2(0) = A(0) = T(0) = L(0) = 0. \tag{11}$$

where N (assumed fixed) is the total number of individuals in the population for the outbreak in question, z is the proportion initially susceptible, I_0 is the given data which is dependent on the population, $R_e = zR_0$ gives the initial effective reproduction number, and $\mu = D/AR$ where AR is the attack rate calculated by $AR = \alpha z(1-e^{-R_0 AR/\alpha})$.

In order to make the reader know how the above formulas come from, we describe every formula (according to the chart at the beginning of Section 1) as follows. Equation (1) describes the variation of the prior immune individuals M, a proportion μ of M were deaths and the remaining became into the susceptible individuals S within the period of time in resistant state T_w, where $T_w = 2/\phi$. The force-of-infection λ is given by $\lambda = \frac{R_0\nu}{N\alpha}I$. Formulas (2) and (3) can be respectively rewritten as $\frac{dS}{dt} = -\lambda S + \phi T$, $\frac{dE_1}{dt} = \lambda S - \gamma E_1$. Formula (2) explains the variation of susceptible individuals S: the increase of S from the recovered individuals with temporary immunity ϕT and the decrease of S because of the force of infection λ. Formula (3) describes the variation of individuals at the first latent state E_1 with the latent infectious rate γ. Formula (4) describes the variation of individuals at the second exposed state E_2 of latent infection. Formula (5) describes the variation of the asymptomatic or unreported infectious individuals A: a proportion $1-\alpha$ of E_2 with the latent infectious rate γ become into A and the recovery rate of A is ν. Similarly as formula (5), formula (6) describes the variation of the remaining proportion α of E_2 which become into the infective and symptomatic class of individuals I, with the recovery rate ν. Formula (7) describes a proportion μ of I become deaths. Formula (8) describes the variation of the recovered individuals R: some I and A individuals recovered with rate ν, but a proportion ϕ of R become into the class of susceptible individuals S again. Formula (9) describes $(1-\rho)\phi$ of R individuals were not susceptible temporarily and a proportion ϕ of the temporary class of individuals T become into S soon. Formula (10) describes $\rho\phi$ of recovered individuals R become into the class of longer-lasting protected individuals L. Formula (11) describes the initial values of the variables. The descriptions of formulas (2)-(11) can be referred to the references such as [5, 8, 9, 10, 12, 17, 20, 21, 22, 37].

2.2 An Simulated Annealing Refined Replica Exchange Markov Chain Monte Carlo Algorithm

MCMC algorithms are sampling from probability distributions based on constructing a Markov chain that has the desired distribution as its equilibrium distribution ([37]). The sampling strategy is very critical for a successful MCMC algorithm. However, in practice, the MCMC sampling methods such as Gibbs sampling, Metropolis-Hastings algorithm ([4]), Multiple-try Metropolis algorithm sometimes just randomly walk and take a long time to explore all the solution space, will often double back and cover ground already covered, and usually own a slow algorithm convergence. In this paper a more efficient sampling strategy of simulated annealing-refined RE is enclosed into the MCMC simulation.

In the Metropolis-Hastings-based MCMC (MHMCMC), a Markov stochastic process is built to sample a target probability $p(x) = C^{-1}e^{-f(x)}$ for a current state x, where $f(x)$ is the objective function (which is the likelihood in this paper) and C denotes the normalization constant. For simulated annealing, a variable temperature $Temp$ is introduced into the objective function of the target distribution, i.e. $p(x) = C^{-1}e^{-f(x)/Temp}$. For RE, a new state y is generated from the current state x of the Markov process by drawing y with a transition probability $q(x, y)$, and the new state y is accepted with the probability $\min(1, [p(y)q(y, x)]/[p(x)q(x, y)])$. In the

RE implementation, for a replica j at each iteration step l, the local Markov chain move from the conformation state x_j^l to the new state x_j^{l+1} accepted with the probability $\min(1, e^{-1/Temp(j)(f(x_j^{l+1})-f(x_j^l))})$, and the replica transition from j to $j+1$ at two neighbouring temperatures $Temp(j)$ and $Temp(j+1)$ with the accepted probability $\min(1, e^{-1/Temp(j)f(x_{j+1}^{l+1})-1/Temp(j+1)f(x_j^{l+1})+1/Temp(j+1)f(x_{j+1}^{l+1})+1/Temp(j)f(x_j^{l+1})})$. The temperatures are monotonically decreasing in order for the convenience of simulated annealing in use and the transition step size of RE is larger for higher temperature and smaller for the lower temperature. The negative binomial distribution is used to calculate the maximum likelihood, where the likelihood is formed by assuming Gaussian errors around the deterministic model. For the simulated annealing refinement for RE, the neignbourhood scheme of [3] is still in use here. The pseudo-code of the simulated annealing refined REMCMC algorithm is presented as follows:

Define random and constant *parameters*
Initialization:
offset =0
for (i=1 to replicas) do

Set up MCMC random and constant *Parameters* for each replica

Temperature scheme to produce *Temp(i)*

MCMC Initialized at *Temp(i)* to get *MSEIRSinit*

endfor
Do MCMC with RE:
for (i_set=1 to Total_set) do

Set(i) of Total_set:

for (j=1 to replicas) do

Input *Parameters* and *MSEIRSinit*

Call MCMC to get new *Parameters* and each likelihood, accepting new MC move with Metropolis criterion for each replica

Output new *Parameters*, and the *Likelihood_last(j)*, *Likelihood_last_cold(j)*

endfor

j = offset +1

while (j+1 $\leq$ replicas) do

k=j+1

$\Delta = (\frac{1}{Temp(k)} - \frac{1}{Temp(j)})$*(*Likelihood_last_cold(j)*$-$*Likelihood_last_cold(k)*)

if ($\Delta \leq 0$) then

Output *Likelihood_last(j)*

swap *Parameters* and Labels of j and k

else

Generate a random number *Rand* of [0,1]

if ($Rand \leq e^{-\Delta}$) then

Output *Likelihood_last(j)*

swap *Parameters* and Labels of j and k

endif

endif

j=j+2

endwhile

offset = 1- offset

endfor

Adjust each of *Temps* by simulated annealing & repeat the algorithm untill reach *Temp_target*.

3 Numerical Results and Discussion

The data used to test the above simulated annealing refined REMCMC (SAREMCMC) algorithm for fitting the extended MSEIRS Model for the transmission of the H1N1 influenza is the mortality data from five English towns (Blackburn, Leicester, Manchester, Newcastle and Wigan) collected during the 1918-19 influenza pandemic ([27]). In the TABLES 1, 2A-2N, 3-5 of [27] pages 136-143, the details of the triple pandemic wave data in 1918-19 of English localities are given. This paper just uses the mortality data (i.e. the 1st, 2nd, 3rd ... 48th week of the deaths of people in each of the five places), which are listed in Table 1.

10 replicas and 10000 iterations are set for the algorithm, Total_set=50. To compare with the SAREMCMC algorithm, the MHMCMC algorithm ([4, 37]) is run for 10000 iterations too. The model curves fitted to the data are shown in Figures 1-5, from which we can see that the model mortality curve well fits the death data for each of the five populations by the SAREMCMC algorithm, but the MHMCMC algorithm can only well fit for the Leicester and Wigan populations. The comparisons of the successful parameter maximum likelihood estimates and credibility intervals calculated by the both algorithms of 10000 iterations are listed in Tables 2-3.

In Tables 2-3 the 95% credibility interval for SAREMCMC is much wider than for MHMCMC. We can see that the upper bound values for z (the proportion susceptible before the summer wave of the all population) are very high (92.1% and 99.7%) for the Leicester and Wigan populations; the upper bound values of α (the proportion of becoming infective and symptomatic) are also very high (96.3% and 99.7% for summer wave, 99.1% and 100% for autumn wave, 99.7% and 99.8% for winter wave) for the Leicester and Wigan populations; this agrees with the assumption of [14, 25, 26] that with a new virus, the entire population is susceptible. However, the local search of MHMCMC conflicts with this assumption. For the both populations, the effective reproduction number R_e is much less than R_0 so that the mortality rate is no more than 3.1% as low as reported ([27]). To further confirm the above observations, the MHMCMC was run 50000 iterations and the MMMCMC (Multiple-try Metropolis Markov Chain Monte Carlo) was run for 14999 iterations. In Figures 1-5 we may see that the performance of MHMCMC of 50000 iterations and of MMMCMC of 14999 iterations are still not better than that of SAREMCMC of 10000 iterations. This further confirms

that REMCMC is much better than MHMCMC and MMMCMC for solving the H1N1 influenza pandemic model.

The detailed analysis for Tables 2-3 is not the interests of this paper because (1) such a complex MSEIRS model is highly over-parameterized with respect to the data and the estimates are highly correlated; (2) the model should consider the rich data of age classes ([27]); and (3) the estimates obtained (such as R_0) need to be properly compared to existing estimates in literatures (e.g. [14, 21, 24]) argued. This will be a further research direction of the author.

4 Conclusion

This paper is concerned with a computational algorithm for fitting the deterministic MSEIRS epidemic model for the transmission of H1N1 influenza to mortality data. The model-fitting is carried out using a simulated annealing refined replica exchange stochastic algorithm. The algorithm is superior to other existing sampling algorithms such as the Gibbs sampling, the Metropolis-Hastings algorithm, the Multiple-try Metropolis algorithm through the illustration of using the triple wave mortality data from five English towns collected during the 1918-19 influenza pandemic. The algorithm presented in this paper has great promise to be used for carrying out some numerical computations of the current complex 2009-10 influenza pandemic.

Acknowledgments: The author appreciates the anonymous referees and editors for the numerous insightful comments (05-JAN-2010) on the original manuscript and further comments (01-MAY-2010) on the revised manuscript, which have improved this paper greatly.

References

[1] Anderson, R., May, R.M. (1992) Infectious diseases of humans: dynamics and control, Oxford University Press, Oxford.

[2] Andrieu, C., De Freitas, N., Doucet, A., Jordan, M.I. (2003) An Introduction to MCMC for machine learning. Mach. Learn. 50, 5–43.

[3] Bagirov, A.M., Zhang, J.P. (2003) Comparative analysis of the cutting angle and simulated annealing methods in global optimization. Opt. 52, 363–378.

[4] Baldi, P., Brunak, S. (2001) Bioinformatics: The Machine Learning Approach (2nd Edition), MIT Press, Chapter 4.5.

[5] Bootsma, M.C.J., Ferguson, N.M. (2007) The effect of public health measures on the 1918 influenza pandemic in U.S. cities. P.N.A.S. USA 104 (18), 7588-93.

[6] Bos, M.E.H. et al (2007) Estimating the day of highly pathogenic avian influenza (H7N7) virus introduction into a poultry flock based on mortality data. Vet. Res., 38, 493–504.

[7] Caley, P., Philp, D.J., McCracken, K. (2008) Quantifying social distancing arising from pandemic influenza. J. R. Soc. Interface 5, 631–9.

[8] Chen, S.C., Chio, C.P., Jou, L.J., Liao, C.M. (2009) Viral kinetics and exhaled droplet size affect indoor transmission dynamics of influenza infection. Indoor Air, 19, 401–13.

[9] Chen, S.C., Liao, C.M. (2008) Modelling control measures to reduce the impact of pandemic influenza among schoolchildren. Epidemiol. Infect., 136, 1035–45.

[10] Chowell, G., Ammon, C.E., Hengartner, N.W., Hyman, J.M. (2006) Transmission dynamics of the great influenza pandemic of 1918 in Geneva, Switzerland: assessing the effects of hypothetical interventions. J. Theor. Bio. 241, 193-204.

[11] Chowell, G., Ammon, C.E., Hengartner, N.W., Hyman, J.M. (2006) Estimation of the reproductive number of the Spanish flu epidemic in Geneva, Switzerland. Vaccine 24, 6747-50.

[12] Chowell, G., Nishiura, H., Bettencourt, L.M.A. (2007) Comparative estimation of the reproduction number for pandemic influenza from daily case notification data. J. R. Soc. Interface 4, 155–66.

[13] Earl, D.J., Deem, M.W. (2005) Parallel tempering: theory, applications, and new perspectives. Phys. Chem. Chem. Phys. 7, 3910–6.

[14] Fraser, C. et al (2009) Pandemic potential of a strain of influenza A (H1N1): early findings. Science 324, 1557-61.

[15] Iba, Y. (2001) Extended ensemble Monte Carlo. Int. J. Mod. Phys. C 12, 623–56.

[16] Kirkpatrick, S., Gelatt, C.D., Vecchi, M.P. (1983) Optimization by simulated annealing. Science 220, 671–80.

[17] Lee, V.J., Chen, M.I. (2007) Effectiveness of neuraminidase inhibitors for preventing staff absenteeism during pandemic influenza. Emerg. Infect. Dis. 13, 449-57.

[18] Li, Y., Protopopescub, V.A., Arnoldc, N., Zhang, X., Gorine, A. (2009) Hybrid parallel tempering and simulated annealing method. App. Math. Comput. 212 (1), 216–28.

[19] Li, Y., Mascagni, M., Gorin, A. (2009) A decentralized parallel implementation for parallel tempering algorithm. Parallel Computing 35, 269-83.

[20] Lunelli, A., Pugliese, A., Rizzo, C. (2009) Epidemic patch models applied to pandemic influenza: contact matrix, stochasticity, robustness of predictions. Mathematical Biosciences 220, 24–33.

[21] Mathews, J.D., McBryde, E.S., McVernon, J., Pallaghy, P.K., McCaw, J.M. (2010) Prior immunity helps to explain wave-like behaviour of pandemic influenza in 1918–9 (& Supplementary material). BMC Infectious Diseases, 10:128.

[22] Mathews, J.D., McCaw, C.T., McVernon, J., McBryde, E.S., McCaw, J.M. (2007) A biological model for influenza transmission: pandemic planning implications of asymptomatic infection and immunity. PLoS ONE 2 (11), e1220.

[23] Mathews, J.D., Chesson, J.M., McCaw, J.M., McVernon, J. (2009) Understanding influenza transmission, immunity and pandemic threats. Influenza and Other Respiratory Virus 3(4), 143-9.

[24] McCaw, J.M., McVernon, J., McBryde, E.S., Mathews, J.D. (2009) Influenza: accounting for prior immunity. Science 325, 1071.

[25] J. Medlock, J., Galvani, A.P. (2009) Optimizing influenza vaccine distribution. Science, 325, 1705–8.

[26] Mills, C.E., Robins J.M., Lipsitch M. (2004) Transmissibility of 1918 pandemic influenza. Nature 432, 904-6.

[27] Ministry of Health (1920) Reports on the pandemic of influenza 1918–1919, Reports on Public Health and Medical Subjects No. 4, Ministry of Health, London, England: His Majesty's Stationery Office.

[28] Nishiura, H. (2007) Time variations in the transmissibility of pandemic influenza in Prussia, Germany, from 1918-19. Theoretical Biology and Medical Modelling 4, 20–29.

[29] Park, A.W. et al (2004) The effects of strain heterology on the epidemiology of equine influenza in a vaccinated population. Proc. R. Soc. Lond. B 271, 1547–55.

[30] Ross, S.M. (2006) Introduction to Probability Models (9th Edition), Elsevier Science & Technology Books Publisher.

[31] Sertsou, G., Wilson, N., Baker1, M., Nelson, P., Roberts, M.G. (2006) Key transmission parameters of an institutional outbreak during the 1918 influenza pandemic estimated by mathematical modelling. Theoretical Biology and Medical Modelling 3, 38–45.

[32] Swendsen, R.H., Wang, J.S. (1986) Replica Monte Carlo simulation of spin-glasses. Phys. Rev. Lett. 57 (21), 2607–9.

[33] Thachuk, C., Shmygelska, A., Hoos, H.H. (2007) A replica exchange Monte Carlo algorithm for protein folding in the HP model. BMC Bioinformatics 8, 342–62.

[34] Viboud, C., Tamb, T., Fleming, D., Handel, A., Miller, M.A., Simonsen, L. (2006) Transmissibility and mortality impact of epidemic and pandemic influenza, with emphasis on the unusually deadly 1951 epidemic. Vaccine 24, 6701-7.

[35] Vynnycky, E., Trindall, A., Mangtani, P. (2007) Estimates of the reproduction numbers of Spanish influenza using morbidity data. International Journal of Epidemiology 36, 881-9.

[36] White, L.F., Pagano, M. (2008) Transmissibility of the influenza virus in the 1918 pandemic. PLoS ONE 3 (1): e1498.

[37] Wikipedia, the free encyclopedia (http://en.wikipedia.org/wiki/): Epidemic model, Compartmental models in epidemiology, Mathematical modelling of infectious disease, Markov chain Monte Carlo, Parallel tempering, Metropolis-Hastings algorithm, etc (and references therein).

Tables and Figures:

Table 1: Mortality data of 1918-19 H1N1 influenza pandemic

Week number\Population	Blackburn	Leicester	Manchester	Newcastle	Wigan
Week 1	0	0	0	0	0
Week 2	0	0	2	0	0
Week 3	0	0	2	0	0
Week 4	0	0	2	0	0
Week 5	0	1	8	1	0
Week 6	6	7	83	30	4
Week 7	21	24	113	45	6
Week 8	15	30	74	27	17
Week 9	13	5	26	12	8
Week 10	2	0	8	5	6
Week 11	3	5	3	1	1
Week 12	0	1	3	0	2
Week 13	3	2	4	0	1
Week 14	1	0	3	2	0
Week 15	0	1	3	0	0
Week 16	0	1	2	0	0
Week 17	0	0	2	0	1
Week 18	0	1	1	0	1
Week 19	0	0	3	1	0
Week 20	0	5	2	1	0
Week 21	0	56	12	12	5
Week 22	2	197	32	7	32
Week 23	10	269	83	32	34
Week 24	29	141	162	81	26
Week 25	25	72	235	73	15
Week 26	42	19	311	101	12
Week 27	49	18	374	99	10
Week 28	47	19	254	68	11
Week 29	36	9	111	41	22
Week 30	15	11	55	15	12
Week 31	11	3	39	15	1
Week 32	3	2	14	7	7
Week 33	2	3	16	6	3
Week 34	3	1	18	3	3
Week 35	1	0	6	3	2
Week 36	1	1	9	11	6
Week 37	1	2	28	42	27
Week 38	9	12	44	119	23
Week 39	33	61	130	163	27
Week 40	46	90	196	94	21
Week 41	50	49	210	58	6
Week 42	15	42	117	33	13
Week 43	12	20	74	22	3
Week 44	2	6	54	15	12
Week 45	4	7	34	4	4
Week 46	0	3	21	7	7
Week 47	1	0	17	6	3
Week 48	2	2	9	2	0

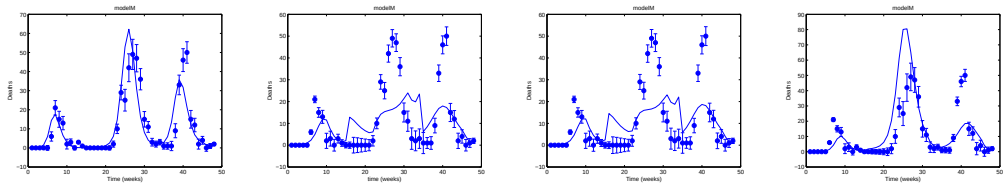

Figure 1: Death data and its fitted model mortality curve for the Blackburn population (from left to right: SAREMCMC (10000 iterations), MHMCMC (10000 iterations), MHMCMC (50000 iterations), MMMCMC (14999 iterations)).

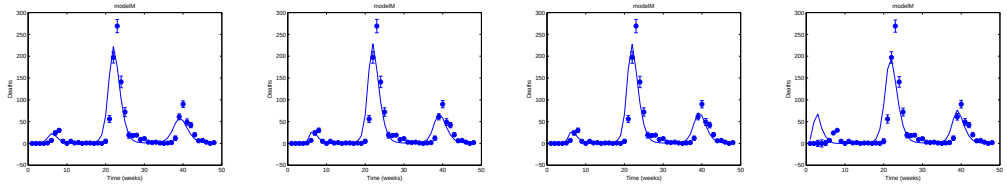

Figure 2: Death data and its fitted model mortality curve for the Leicester population (from left to right: SAREMCMC (10000 iterations), MHMCMC (10000 iterations), MHMCMC (50000 iterations), MMMCMC (14999 iterations)).

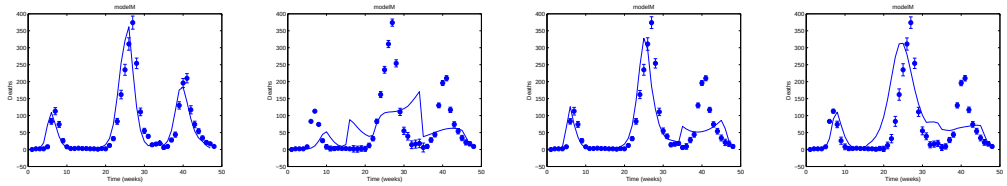

Figure 3: Death data and its fitted model mortality curve for the Manchester population (from left to right: SAREMCMC (10000 iterations), MHMCMC (10000 iterations), MHMCMC (50000 iterations), MMMCMC (14999 iterations)).

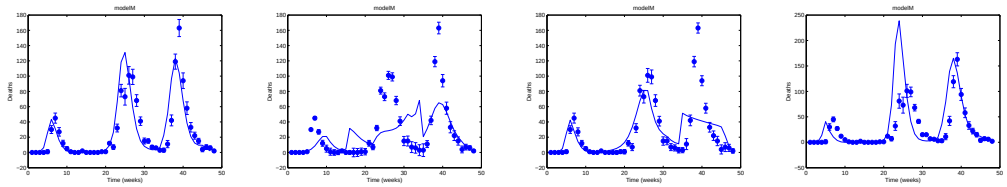

Figure 4: Death data and its fitted model mortality curve for the Newcastle population (from left to right: SAREMCMC (10000 iterations), MHMCMC (10000 iterations), MHMCMC (50000 iterations), MMMCMC (14999 iterations)).

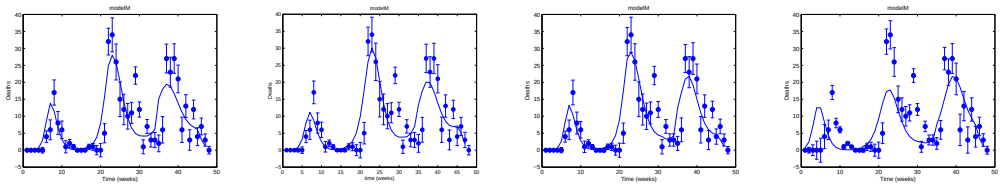

Figure 5: Death data and its fitted model mortality curve for the Wigan population (from left to right: SAREMCMC (10000 iterations), MHMCMC (10000 iterations), MHMCMC (50000 iterations), MMMCMC (14999 iterations)).

Table 2: Successful parameters and summary statistics for the Leicester population

Estimated quantity	SAREMCMC	MHMCMC
R_0	6.530 (1.076, 9.747)	4.131 (4.055, 4.695)
$\log T_w$	4.412 (1.029, 11.293)	5.163 (4.945, 5.558)
ρ	0.427 (0.036, 0.976)	0.366 (0.307, 0.672)
z	0.454 (0.106, 0.921)	0.313 (0.235, 0.367)
$\frac{1}{\nu}$ (mean infective period (days))	1.201 (0.642, 2.969)	1.204 (0.971, 1.264)
b_1 (seasonal forcing)	0.121 (0.002, 0.239)	0.153 (0.055, 0.183)
T_{seed_2} (the time of between summer and autumn waves)	114.609 (90.478, 139.623)	120 (105, 125)
T_{seed_3} (the time of between autumn and winter waves)	275.726 (181.750, 321.726)	196 (189, 223)
T_{seed_1} (the time before the summer wave)	44.858 (2.030, 52.467)	39 (28, 42)
$\log T_w M$	6.461 (0.062, 11.261)	4.937 (4.645, 5.520)
α_1 (summer wave)	0.168 (0.069, 0.997)	0.127 (0.107, 0.201)
α_2 (autumn wave)	0.821 (0.389, 1.000)	0.405 (0.399, 0.499)
α_3 (winter wave)	0.644 (0.228, 0.997)	0.256 (0.246, 0.391)
μ_1 (summer wave)	0.006 (0.003, 0.007)	0.005 (0.004, 0.006)
μ_2 (autumn wave)	0.029 (0.022, 0.037)	0.026 (0.023, 0.029)
μ_3 (winter wave)	0.019 (0.014, 0.023)	0.017 (0.015, 0.020)
Serial interval $\frac{2}{\gamma} + \frac{1}{\nu}$ (days)	2.501 (1.942, 4.269)	2.430 (2.271, 2.564)
Doubling time in fully susceptible population (days)	0.636 (0.484, 19.622)	0.892 (0.788, 0.944)
Doubling time in actual population (days)	0.907 (-130.666, 278.363)	4.340 (-14.687, 17.965)
Infections per person per day in fully susceptible population	5.851 (0.437, 9.673)	2.430 (2.271, 2.564)
Infections per person per day in actual population	2.743 (0.046, 5.976)	1.269 (0.845, 1.495)

Notes: Parameter values (maximum likelihood value, 95% credibility intervals) were estimated by the SAREMCMC and MHMCMC simulations of 10000 iterations. The estimate for the serial interval, doubling time and infections per day per transmitter (median, 95% credibility intervals) were derived from the full SAREMCMC distributions. $\frac{1}{\nu}$: mean infective period (days). b: seasonal forcing. T_{seed_2}: the time of between summer and autumn waves. T_{seed_3}: the time of between autumn and winter waves. T_{seed_1}: the time before the summer wave. Serial Interval: $\frac{2}{\gamma} + \frac{1}{\nu}$ (days). DTFS: Doubling Time in Fully Susceptible population (days). DTA: Doubling Time in Actual population (days). IFS: Infections per person per day in Fully Susceptible population. IA: Infections per person per day in Actual population.

Table 3: Successful parameters and summary statistics for the Wigan population

Estimated quantity	SAREMCMC	MHMCMC
R_0	3.884 (1.079, 8.448)	4.830 (3.756, 5.743)
$\log T_w$	5.314 (0.277, 11.345)	3.925 (3.660, 4.100)
ρ	0.476 (0.017, 0.984)	0.268 (0.011, 0.481)
z	0.277 (0.020, 0.997)	0.323 (0.281, 0.398)
$\frac{1}{\nu}$ (mean infective period (days))	1.175 (0.720, 2.957)	1.195 (0.798, 1.824)
b_1 (seasonal forcing)	0.053 (0.001, 0.248)	0.031 (0.002, 0.072)
T_{seed_2} (the time of between summer and autumn waves)	109.518 (90.442, 139.347)	93 (90, 138)
T_{seed_3} (the time of between autumn and winter waves)	265.731 (185.367, 314.367)	244 (213, 269)
T_{seed_1} (the time before the summer wave)	12.913 (2.109, 54.464)	29 (20, 37)
$\log T_w M$	6.489 (0.300, 11.247)	7.228 (6.934, 9.029)
α_1 (summer wave)	0.294 (0.025, 0.963)	0.201 (0.132, 0.295)
α_2 (autumn wave)	0.564 (0.204, 0.991)	0.419 (0.337, 0.607)
α_3 (winter wave)	0.634 (0.313, 0.998)	0.572 (0.429, 0.753)
μ_1 (summer wave)	0.013 (0.008, 0.018)	0.011 (0.009, 0.017)
μ_2 (autumn wave)	0.031 (0.021, 0.042)	0.030 (0.022, 0.040)
μ_3 (winter wave)	0.019 (0.014, 0.023)	0.019 (0.016, 0.023)
Serial interval $\frac{2}{\gamma} + \frac{1}{\nu}$ (days)	2.475 (2.020, 4.257)	2.390 (2.098, 3.124)
Doubling time in fully susceptible population (days)	0.894 (0.525, 24.754)	0.779 (0.685, 1.157)
Doubling time in actual population (days)	4.612 (-36.995, 96.889)	3.717 (2.774, 4.705)
Infections per person per day in fully susceptible population	4.143 (0.428, 8.402)	4.574 (2.200, 5.813)
Infections per person per day in actual population	0.991 (0.112, 3.818)	1.423 (0.850, 1.814)

Notes: Parameter values (maximum likelihood value, 95% credibility intervals) were estimated by the SAREMCMC and MHMCMC simulations of 10000 iterations. The estimate for the serial interval, doubling time and infections per day per transmitter (median, 95% credibility intervals) were derived from the full SAREMCMC distributions. $\frac{1}{\nu}$: mean infective period (days). b: seasonal forcing. T_{seed_2}: the time of between summer and autumn waves. T_{seed_3}: the time of between autumn and winter waves. T_{seed_1}: the time before the summer wave. Serial Interval: $\frac{2}{\gamma} + \frac{1}{\nu}$ (days). DTFS: Doubling Time in Fully Susceptible population (days). DTA: Doubling Time in Actual population (days). IFS: Infections per person per day in Fully Susceptible population. IA: Infections per person per day in Actual population.